JOURNAL OF SOLID STATE CHEMISTRY 103, 95–104 (1993)

Physico-chemical Characterizations of Au(III) in $Ln_2Li_{0.50}Au_{0.50}O_4$ (*Ln* = La, Nd, Sm, Eu, Gd) Oxides

F. TRESSE, G. DEMAZEAU, J. P. SANCHEZ,* L. FOURNES, AND K. S. SUH

*Laboratoire de Chimie du Solide du CNRS and Interface Hautes Pressions, ENSCPB–Université Bordeaux I, 33405 Talence Cedex, France; and *CENG–DRFMC/SPSMS/LIH, 85X, 38041 Grenoble Cedex, France*

Received November 1, 1991; in revised form August 3, 1992; accepted August 10, 1992

The $Ln_2Li_{0.50}Au_{0.50}O_4$ (*Ln* = La, Nd, Sm, Eu, Gd) oxides have been prepared under oxygen pressure. The physical and chemical characterizations of the lanthanum phase confirm the stabilization of trivalent gold in a square-planar surrounding. Lithium is located in two similar crystallographic sites, in agreement with a layered structure with a 1/1 cationic order in the layers. The crystal structure is discussed, but the absence of single-crystal data does not allow a precise determination.

I. Introduction

In the Li–*M*–O system (*M* = transition elements), when the Li–*M*–O angle is close to 180° the high ionicity of Li–O bonds reinforces the covalency of the antagonist-bonds which share the same oxygen 2*p* orbital. A regular distribution of the weak Li–O bonds surrounding the (MO_6) octahedron has been used for stabilizing the isotropic electronic configuration in a perovskite-type lattice. This is the case of Ru(V), Os(V) (*1*), or Fe(V) (*2*) d^3 in the La_2LiMO_6 oxides.

If Li–O bonds are only located in the *x*O*y* planes of the K_2NiF_4-type structure, it is possible to stabilize some anisotropic electronic configurations such high-spin (HS) Fe(IV) ($t_{2g}^3 d_{z^2}^1 d_{x^2-y^2}^0$) in $A_{0.50}La_{1.50}Li_{0.50}Fe_{0.50}O_4$ (*A* = *Ca*, *Sr*, *Ba*) (*3*) and low-spin (LS) Ni(III) ($t_{2g}^6 d_{z^2}^1 d_{x^2-y^2}^0$) in $La_2Li_{0.50}Ni_{0.50}O_4$ (*4*).

The stabilization of high oxidation states of transition elements in different oxygenated lattices allows the study of correlations between the physical properties of such materials versus the metal–oxygen bonding strength (*5*).

Numerous unusual oxidation states or electronic configurations of the first family of transition elements (3*d*) have been characterized in oxides such as high-spin Fe(IV) in $A_{0.50}La_{1.50}Li_{0.50}Fe(IV)_{0.50}O_4$ (*A* = Ca, Sr, Ba) (*3*), Fe(V) in $La_2LiFe(V)O_6$ (*2*), the LS → HS transition of Co(III) in *Ln*Co(III)O_3 (*Ln*(III) = rare-earth) (*6–9*), the intermediate spin state (*S* = 1) of Co(III) in $La_2Li_{0.50}Co(III)_{0.50}O_4$ (*10*) and $La_2Li_{0.50}Cu(III)_{0.50-x}Co(III)_xO_4$ (*11*), LS Co(IV) in $Sr_{0.50}La_{1.50}Li_{0.50}Co(IV)_{0.50}O_4$ (*12*), LS Ni(III) in *Ln*Ni(III)O_3 (*13–16*) and Sr*Ln*Ni(III)O_4 (*17*) (*Ln*(III) = rare-earth), Cu(III) in LaCu(III)O_3 (*18*), and d^8(LS) Cu(III) in $La_2Li_{0.50}Cu(III)_{0.50}O_4$ (*18*) and SrLaCu(III)O_4 (*19*). Few transition elements of the second (4*d*) and third (5*d*) se-

0022-4596/93 $5.00

ries have been studied. However, Ru(V) in $La_2LiRu(V)O_6$ (*1*), Pd(IV) in $Zn_2Pd(IV)O_4$ (*20*), Ir(V) in $La_2LiIr(V)O_6$ (*1*, *21*, *22*), and Pt(IV) in $Mg_2Pt(IV)O_4$ (*23*) have been found.

The superconducting oxides are characterized by a mixed valence, low-dimensional structure containing polyhedron of variable coordinations. The stabilization and the study of transition elements in different oxygen coordinations were able to lead us to a better understanding of the superconducting behavior (*24*, *25*).

In oxides lattices Cu(II)(d^9) and Cu(III)(d^8) can adopt several different coordinations such as (i) more or less distorted octahedral (La_2CuO_4 (*26*) and $La_2Li_{0.50}Cu_{0.50}O_4$ (*18*)), (ii) square-planar (Nd_2CuO_4 (*27*)), and (iii) pyramidal with a square base ($YBa_2Cu_3O_7$ (*28*), $Nd_{2-x-y}Ce_xSr_yCuO_{4-\delta}$ (*29*)).

Gold and silver belong to the same column of the periodic table as copper, but differ by the low stability of the divalent oxidation state. In the case of gold, the oxidation states +I(d^{10}) and +III(d^8) are more stable than +II(d^9). For Au(III), the d^8 low-spin state is stabilized through the covalency of the Au(III)–O bond, such an electronic configuration generally inducing a square-planar coordination. Few oxygenated lattices containing Au(III) have been prepared, namely, $A\,AuO_2$ (A = Na, K, Rb, Cs) (*30*). In these structures, Au(III) adopts square-planar (AuO_4) coordination, forming sheets by edge sharing (Fig. 1). In order to investigate isolated Au(III), we have prepared and studied the $Ln_2Li_{0.50}Au(III)_{0.50}O_4$ phases (Ln = La, Nd, Eu, Sm, Gd).

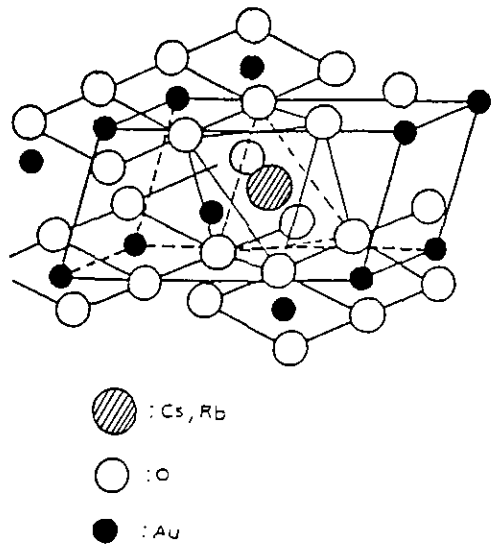

FIG. 1. Square-planar ($AuO_4^{(-V)}$) environment in $RbAu(III)O_2$ and $CsAu(III)O_2$, after H.-D. Wasel-Nielen and R. Hoppe (*30*).

II. Preparation of the Materials

Two different methods have been used for the preparation of the $Ln_2Li_{0.50}Au_{0.50}O_4$ phases.

(*a*) *Direct synthesis under oxygen pressure.* Ln_2O_3, Au_2O_3–nH_2O ($n \simeq 2$) were mixed with excess Li_2O_2 compensating the mechanical decomposition of the gold oxide (Au_2O_3 begins to evolve oxygen at 110°C) in the mortar. The lithium peroxide is used in excess due to because of easy sublimation at normal pressure of Li_2O at 923 K. The resulting powders are treated under 70 MPa of oxygen pressure at 1023 K for 12 hr.

Under these experimental conditions, only the phases containing La, Nd, or Sm could be prepared. $Eu_2Li_{0.50}Au_{0.50}O_4$ and $Gd_2Li_{0.50}Au_{0.50}O_4$ were not isolated as pure phases even if the pressure was increased using very high oxygen pressure conditions in a "Belt"-type apparatus (decomposition of $KClO_3$ in the presence of Ln_2O_3, Au_2O_3–nH_2O and Li_2O_2 under 5 GPa (50 kbar), at 1023 K). After the synthesis the excess of Li in the product present as $LiOH \cdot 2H_2O$ could be leached out rapidly with distillated water at pH = 7.

(*b*) *Synthesis in air and sintering under oxygen pressure.* The second method was used only for $La_2Li_{0.50}Au_{0.50}O_4$. It consists

of two successive steps. The first one is a thermal treatment in air at 1023 K of La_2O_3, Au_2O_3–nH_2O, and Li_2O_2 (in 1200% mass excess). After 15 hr of thermal treatment, the mixture, contained in an alumina crucible, is quenched in air to room temperature. The excess of lithium is eliminated by a distilled-water washing as previously described. The resulting product is dryed at 400 K for 5 hr in order to eliminate the absorbed water, followed by a second treatment under 80 MPa of oxygen pressure at 773 K for 15 hr in a gold tube. The second method leads to a well crystallized material. The occurrence of $LaLiO_2$ in same preparations at higher temperatures seems to indicate a partial reduction of the gold oxide, leading to a deficiency of this element. The gold phases $Ln_2Li_{0.50}Au_{0.50}O_4$ (Ln = La, Nd, Sm) are pale-yellow colored.

III. Experimental Results

(*a*) *Determination of the gold oxidation state.* Iodometric titration has been performed and leads to an average oxidation state close to 3+ for gold in such oxides.

(*b*) *X-ray diffraction study.* The X-ray diffraction pattern (XRDP) of $La_2Li_{0.50}Au_{0.50}O_4$, $Nd_2Li_{0.50}Au_{0.50}O_4$, and $Sm_2Li_{0.50}Au_{0.50}O_4$ are given in Fig. 2. The two first patterns have been indexed in the *Cmmm* space group as proposed by F. Abbattista *et al.* (*31*) for the lanthanum phase. The chosen cell parameters a, b, and c with $a = c = a_0\sqrt{2}$ and $b = c_0$; a_0 and c_0 being the parameters of the base K_2NiF_4-type tetragonal cell. Such an indexation could be induced by a 1/1 Li(I)/Au(III) order in the xOy planes, probably due to the large charge difference between these cations. The $Sm_2Li_{0.50}Au_{0.50}O_4$ structure belongs to a K_2NiF_4-type, but the space group could not be determined.

The cell parameters of these three phases are given in Table I. The c_0/a_0 ratio is close to 3.05 for La and Nd phases and 3.10 for the Sm phase. In layered structures and more specially, those deriving from K_2NiF_4-type, the c_0/a_0 ratio should be correlated with the local distortion of the cationic coordination polyhedron.

It is notable that the experimental c_0/a_0 values for the three phases are lower than those observed for the K_2NiF_4-type oxides.

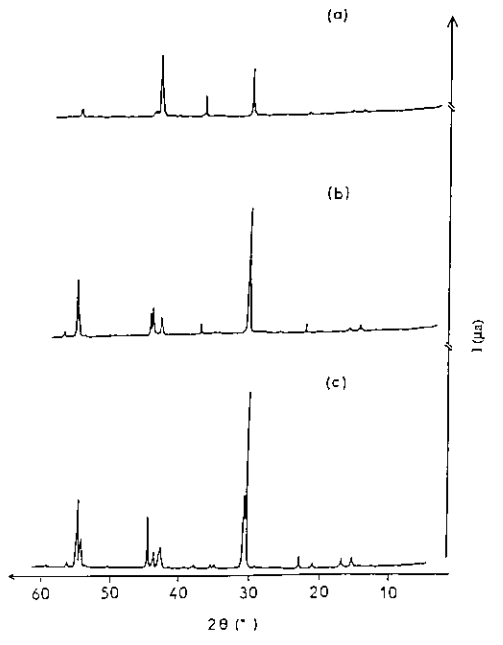

FIG. 2. X-ray diffraction patterns of: (a) $Sm_2Li_{0.50}Au_{0.50}O_4$, (b) $Nd_2Li_{0.50}Au_{0.50}O_4$, and (c) $La_2Li_{0.50}Au_{0.50}O_4$.

TABLE I

CELL PARAMETERS OF $Ln_2Li_{0.50}Au_{0.50}O_4$ (Ln = La, Nd, Sm) PHASES

	a_0 (Å)	c_0 (Å)	c_0/a_0
$La_2Li_{0.50}Au_{0.50}O_4$	4.07	12.41	3.05
$Nd_2Li_{0.50}Au_{0.50}O_4$	3.98	12.11	3.04
$Sm_2Li_{0.50}Au_{0.50}O_4$	3.92	12.18	3.11

Note. $\mathbf{a} = \mathbf{a}_0 + \mathbf{b}_0$, $\mathbf{b} = \mathbf{c}_0$, and $\mathbf{c} = \mathbf{a}_0 - \mathbf{b}_0$ with $|\mathbf{a}| = \sqrt{2}\,|\mathbf{a}_0|$ and $|\mathbf{a}_0| = |\mathbf{b}_0|$. a_0 and c_0 are the cell parameters of the K_2NiF-type phase, a and b are the parameters of the fundamental cell describing the Li/Au order.

When the transition element is characterized by an isotropic electronic configuration, c_0/a_0 is close to 3.30 ± 0.05 [SrLaFe(III)O_4, with Fe(III) ($t_{2g}^3 e_g^2$), c_0/a_0 = 3.28 (*32*) and $La_2Li_{0.50}Co(III)_{0.50}O_4$ where, at low temperature, Co(III) adopts a low-spin configuration, ($t_{2g}^6 e_g^0$), c_0/a_0 = 3.34 (*10*)]. With a transition ion characterized by an anisotropic electronic configuration, two possibilities could occur: either the difference of the electronic population between the two e_g-type orbitals is (i) one electron (Jahn–Teller distortion), for example, $La_2Li_{0.50}Ni(III)_{0.50}O_4$ (*4*) [low-spin Ni(III), ($t_{2g}^6 d_{z^2}^1$) with $c_0/a_0 \simeq 3.43$], $Sr_{0.50}La_{1.50}Li_{0.50}Fe(IV)_{0.50}O_4$ (*3*) [high-spin Fe(IV) ($t_{2g}^3 d_{z^2}^1$), with $c_0/a_0 \simeq 3.46$)], or (ii) two electrons [low-spin d^8 Cu(III) ($t_{2g}^6 d_{z^2}^2 d_{x^2-y^2}^0$), in $La_2Li_{0.50}Cu(III)_{0.50}O_4$ (*18*) with $c_0/a_0 \simeq 3.54$] (Table II). The low c_0/a_0 values observed for these gold oxides can be compared to those of Ln_2CuO_4 compounds (*27*) (Nd_2CuO_4-type) ($c_0/a_0 \simeq 3.08$) where Cu(II) ($t_{2g}^6 d_{z^2}^2 d_{x^2-y^2}^1$) are in edge-shared square-planar environment (Fig. 3).

(*c*) *Magnetic characterization.* The $La_2Li_{0.50}Au_{0.50}O_4$ phase is diamagnetic at room temperature. This diamagnetic behavior illustrates the pairing of the *d* electrons which should confirm a d^8 low-spin electronic configuration from Au(III).

If, as it has been suggested by the magnetic susceptibility measurements, Au(III) adopts a low-spin d^8 configuration, a low value c_0/a_0 for the $Ln_2Li_{0.50}Au(III)_{0.50}O_4$ phases (*Ln* = La, Nd, Sm) is not compatible with a high elongation of the octahedron (MO_6) (as observed for $La_2Li_{0.50}Cu(III)_{0.50}O_4$ ($c_0/a_0 \simeq 3.54$) where a 1/1 Li/Cu order is assumed in the perovskite-type layers of the K_2NiF_4 lattice). On the other hand, the c_0/a_0 ratio found for $La_2Li_{0.50}Au(III)_{0.50}O_4$ is close to that observed for Nd_2CuO_4 and suggests a square-planar oxygen environment for Au(III). In order to confirm the oxidation state of gold and to precisely determine its oxygen environment, a Mössbauer spectroscopy study has been undertaken.

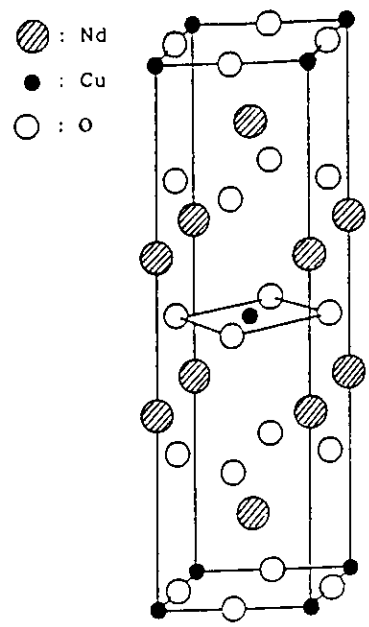

FIG. 3. The Nd_2CuO_4-type structure.

TABLE II

c_0/a_0 RATIO FOR DIFFERENT K_2NIF-TYPE PHASES

Phases	c_0/a_0	Elec. conf.	Ref.
$K_2Ni(II)F_4$	3.26	d^8	(*35*)
$La_2Li_{0.50}Al(III)_{0.50}O_4$	3.38	d^0	(*36*)
$La_2Li_{0.50}Mn(III)_{0.50}O_4$	3.42	d^4	(*37*)
$La_{1.75}Li_{0.75}Fe(IV)_{0.50}O_4$	3.43	d^4	(*38*)
$La_2Li_{0.50}Co(III)_{0.50}O_4$	3.34	d^6	(*10*)
$La_2Li_{0.50}Ni(III)_{0.50}O_4$	3.43	d^7	(*4*)
$La_2Li_{0.50}Cu(III)_{0.50}O_4$	3.54	d^8	(*18*)

(*d*) *Mössbauer study.* ^{197}Au Mössbauer spectroscopy measurements were performed using a ^{197}Pt source obtained by neutron irradiation of 250 mg of natural platinum during 5 hours in a flux of 10^{12}n · cm^2 · sec^{-1}. The absorber thickness was about 90 mg of Au/cm^2. The 77.35 keV gamma rays were detected using an intrinsic high-resolution Ge detector. Both the

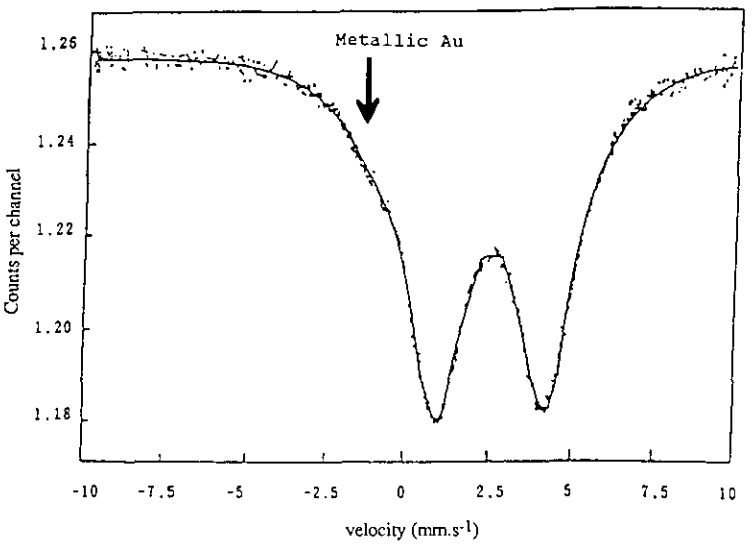

FIG. 4. Mössbauer resonance spectrum of ^{197}Au in $Nd_2Li_{0.50}Au_{0.50}O_4$ at 4.2 K.

source and the absorber were maintained at 4.2 K. The spectrum shown in Fig. 4 was computer analyzed as a superposition of a quadrupole split doublet and a single line. The relevant least-squares fitted parameters are given in Table III. The doublet, which represents about 94% of the spectral area, is characterized by an isomer shift (δ) of 3.75(2) mm · sec^{-1} (versus metallic Au) and a quadrupole splitting (Δ) of 3.28(2) mm · sec^{-1}. As demonstrated previously neither the isomer shift nor the quadrupole splitting values alone can characterize the oxidation state of Au. However, when the two hyperfine parameters are considered together, a clear cut between Au(I) and Au(III) oxidation states can be made (*33*) and Mössbauer spectroscopy of ^{197}Au has been shown to be a valuable tool for characterizing new gold compounds. The Mössbauer data of ^{197}Au in $Nd_2Li_{0.50}Au_{0.50}O_4$ (Table III) demonstrate the occurrence of four coordinates Au(III) which is expected to be in a square-planar oxygen environment (Fig. 5). In this case Au(III) would adopt a d^8 low spin electronic configuration ($t_{2g}^6 d_{z^2}^2 d_{x^2-y^2}^0$), owing to the high covalency of the Au(III)–O bonds. The observed additional single line (about 6% of the total spectral area) is attributed to metallic gold, probably induced by the thermal decomposition of the starting gold oxide material.

TABLE III

MÖSSBAUER PARAMETERS OF ^{197}Au IN $Nd_2Li_{0.50}Au_{0.50}O_4$ AT 4.2 K

	δ (mm · sec^{-1})	Δ (mm · sec^{-1})	W (mm · sec^{-1})	P (%)
Au(III)	3.75(2)	3.28(2)	2.18(2)	94(1)
Au(0)	0.002(2)	0	1.94(11)	6(1)

Note. δ = isomer shift with respect to metallic Au; Δ = quadrupole splitting; W = linewidth of the Lorentzians; P = relative spectral area.

In addition, ^{151}Eu Mössbauer measurements at room temperature of the isotypic $Nd_{1.50}Eu_{0.50}Li_{0.50}Au_{0.50}O_4$ have been performed using a $^{151}SmF_3$ source (Fig. 6). The Mössbauer spectrum consists of a single resonance line. Its isomer (δ) shift of 0.90(2) mm · sec^{-1} (relative to EuF_3) characterizes the occurrence of Eu(III).

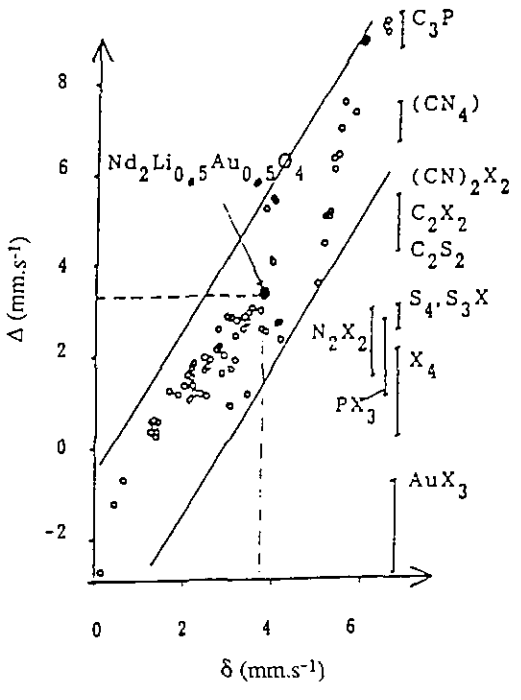

FIG. 5. Correlation diagram of the Mössbauer parameters for some materials containing Au in different polyhedra.

(*e*) *^{7}Li-NMR study of $La_2Li_{0.50}Au_{0.50}O_4$.* An NMR study was performed by Bruker MSL-200 spectrometer with standard variable-temperature unit (VT-1000) to determine the lithium environments in the $La_2Li_{0.50}Au_{0.50}O_4$ phase.

A nucleus of ^{7}Li with $I = 3/2$ in the $La_2Li_{0.50}M(III)_{0.50}O_4$ oxides (M = Co, Ni, Cu) (*34*) is sensitive to the electrostatic environment and the symmetry of the neighbouring sites ($M(III)O_6$) through the quadrupolar interaction with the electric field gradient (g). Spectrometer operating conditions for static spectra are the following:

resonance frequence	77.727 MHz
offset frequency	51,000 Hz
data size	4 K
data point	2 K
spectral width	250 kHz
filter width	500 kHz
pulse program	quadrupole-Echo sequence ($90°_x$-τ-$90°_y$-with 8 cycles) 90° pulse width: 2,4 ≪ s ringdown delay: 12 ≪ s recycle time: 5 sec

The observed results lead to three main conclusions:

(i) the quadrupolar resonance line is not observed down to 195 K,

(ii) only a single narrow line with FWHM (full width at half-maximum) smaller than 750 Hz is observed at room temperature,

(iii) the lines is broadened as decreasing temperature. These results are quite different than those found for the $La_2Li_{0.50}M(III)_{0.50}O_4$ phases (M = Co, Ni, Cu) (*34*), where lithium was characterized by a quadrupolar interaction of 45 to 50 kHz, a value consistent with the structural distortion of the neighboring ($M(III)O_6$) octahedral sites, induced either by the Jahn–Teller distortion due to the low-spin state of Ni(III) or the d^8 low-spin configuration of Cu(III). This site deformation for M(III) atoms increases from Co(III) to Cu(III) and

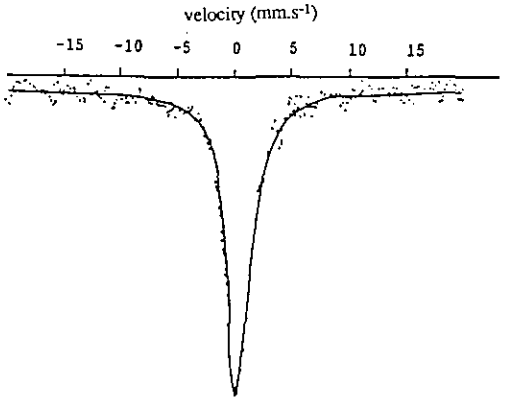

FIG. 6. Mössbauer resonance spectrum of ^{151}Eu in $Nd_{1.50}Eu_{0.50}Li_{0.50}Au_{0.50}O_4$ at 293 K.

could be linked to the electronic configuration of the M(III) at 293 K: low-spin Co(III) ($t_{2g}^6 d_g^0$), low-spin Ni(III) ($t_{2g}^6 d_{z^2}^1$), and d^8 low-spin Cu(III) ($t_{2g}^6 d_{z^2}^2$).

For the $La_2Li_{0.50}Au(III)_{0.50}O_4$ phase, the analysis of the ^7Li NMR spectrum at 293 K leads to two types of possible informations. The very small width of the resonating line ($\simeq$ 750 Hz compared to the 1500 Hz in the case of $La_2Li_{0.50}Cu(III)_{0.50}O_4$ (*34*)) could be due to either a lithium environment different from an elongated octahedron or the relative mobility of this ion in the lattice. The lack of any detectable ionic conductivity on a pellet of sintered $La_2Li_{0.50}Au(III)_{0.50}O_4$ eliminates a possibility of Li(I) mobility. The symmetry of the resonating absorption line indicates a highly symmetric oxygenated site for Li(I). The X-ray diffraction pattern shows no structural transition between 293 and 77 K, thus the thermal evolution of the FWHM of ^7Li NMR line is not correlated to any sizeable modification of the cationic environment (see Fig. 7).

A high-resolution ^7Li NMR study using

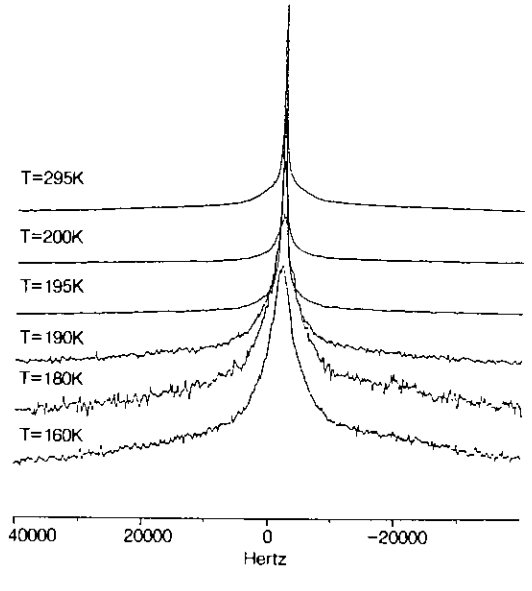

FIG. 7. ^7Li NMR spectra of $La_2Li_{0.50}Au_{0.50}O_4$ versus temperature.

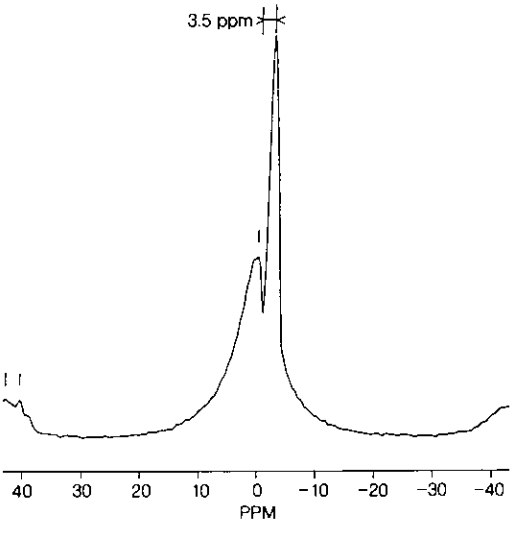

FIG. 8. ^7Li NMR M.A.S. spectrum of $La_2Li_{0.50}Au_{0.50}O_4$.

M.A.S. technique (ν_{rot} = 5 kHz) has been done in order to determine the room-temperature Li-site environment. The spectra is given in Fig. 8. Two different sites ($\delta \simeq$ 3.5 ppm) have been observed in a ratio close to 1/1. This was confirmed by the shape of the rotation bands. Moreover, the significant intensity of the two lines rules out the possibility of an impurity contribution not detected by X-ray diffraction.

In the layered structure of the K_2NiF_4-type characterized by a 1/1 cationic order in the xOy planes, two cationic sites have already been postulated for the transition element (see, for example, the Mössbauer study of $Sr_{0.50}La_{1.50}Li_{0.50}Fe(IV)_{0.50}O_4$ (*3*)). These two sites are induced by stacking faults along the c-axis for the perovskite-type layers containing Li(I) and Fe(IV) (Fig. 9). In the case of $La_2Li_{0.50}Au(III)_{0.50}O_4$, two types of layers could be considered: layers with a mixed Li(I) and Au(III) characterized by a 1/1 cationic order, or layers containing either Li(I) or Au(III).

If we allow a 50% probability that a Li(I) cation (or a Au(III)) is up to a Li(I) taken as

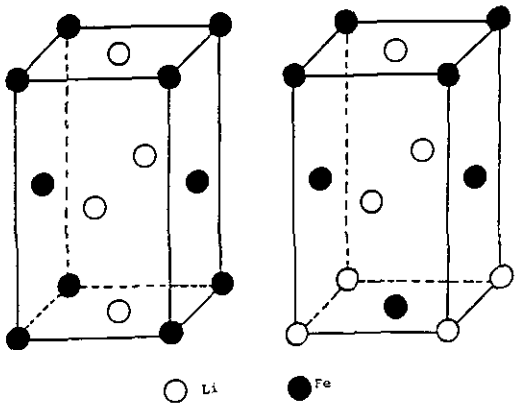

FIG. 9. Schematic representation of the two possible stacking of the (Li/Fe) layers in $Sr_{0.50}La_{1.50}Li_{0.50}Fe_{0.50}O_4$.

reference in a K_2NiF_4-type lattice, these two stacking possibilities lead only to two types of sites (similar to the $Sr_{0.50}La_{1.50}Li_{0.50}Fe(IV)_{0.50}O_4$ lattice), (Fig. 9).

IV. Conclusions

The different physical and chemical characterizations of the $La_2Li_{0.50}Au_{0.50}O_4$ phase, suggest then following points: (i) iodometric titration and Mössbauer study show that gold adopts an oxidation state 3+, (ii) Au(III) is stabilized in an oxygenated square-planar environment (Mössbauer characterization), an elongated octahedral site (AuO_6) is not compatible with the low c_0/a_0 value observed (3.05 compared to 3.54 for $La_2Li_{0.50}Cu(III)_{0.50}O_4$), and (iii) Li(I) is located in two different sites (very close from a crystallographical point of view). Such a result is in good agreement with a layered structure with the Li(I) and Au(III) cations distributed in the same layers (^{7}Li NMR MAS study) with a 1/1 ordering.

At the present stage, it is not possible to precise determination of the Li(I) environment. A more detailed ^{7}Li NMR study should be performed. Moreover, it seems

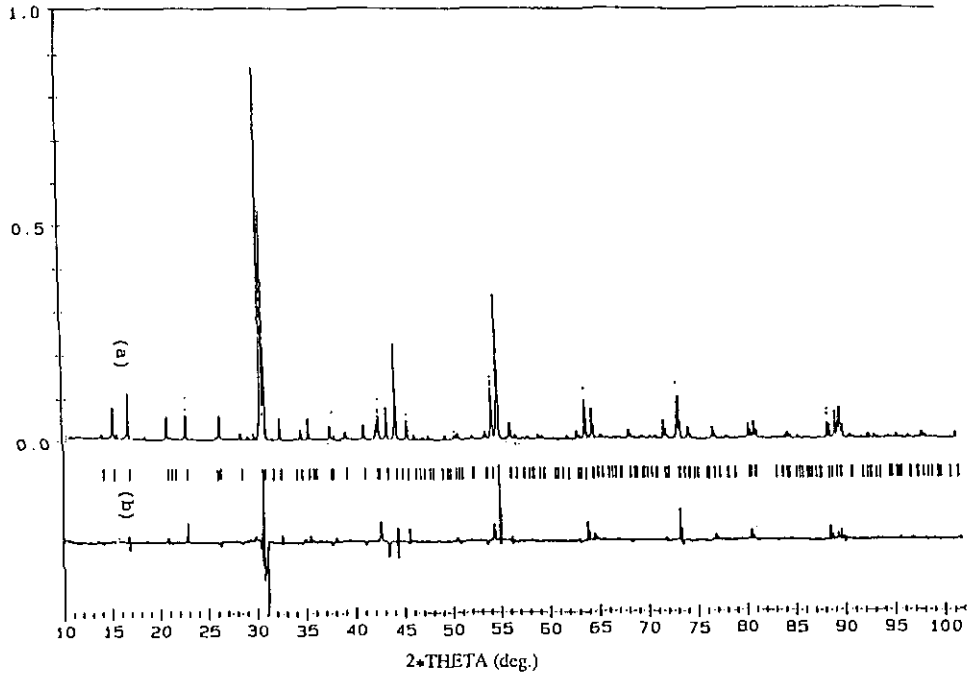

FIG. 10. X-ray diffraction pattern of $La_2Li_{0.50}Au_{0.50}O_4$.

highly probable that the Li site is isotropic but not octahedral. This fact could explain the poor agreement of the structure proposed by F. Abbattista *et al.* (*31*) for $La_2Li_{0.50}Au_{0.50}O_4$ with our X-ray diffraction study performed at room temperature from a step-by-step diffractometer (Fig. 10).

From a Rietveld calculation, the Nd_2CuO_4-type structure gives a better agreement with the experimental data. The lack of reliable information on the Li(I) environment does not allow a precise determination of the real structure, which is probably intermediate between the K_2NiF_4- and Nd_2CuO_4-types. The low Z-values of lithium and oxygen atoms, compared to those of La and Au, using X-ray diffraction, increases the difficulty of solving this structure. Due to the difficulty of preparing a single crystal of such $Ln_2Li_{0.50}Au(III)_{0.50}O_4$ oxides, a neutron powder diffraction study and an enlarged ^7Li investigation are in progress in order to precisely determination the Li(I) environment and the structure.

References

1. K. Hayashi, G. Demazeau, and M. Pouchard, *C. R. Acad. Sci. Paris* **292,** 1433 (1981).
2. B. Buffat, Thèse de l'Université Bordeaux I (France), no. 802 (1984).
3. G. Demazeau, N. Chevreau, L. Fournes, J. L. Soubeyroux, Y. Takeda, M. Thomas, and M. Pouchard, *Rev. Chim. Miner.* **20,** 155 (1983).
4. G. Demazeau, J. L. Marty, M. Pouchard, T. Rojo, J. M. Dance, and P. Hagenmuller, *Mater. Res. Bull.* **16,** 47 (1981).
5. G. Demazeau, *in* "High Pressure Chemical Synthesis" (J. Jurczak and B. Baranowski, Eds.), Chap. 5, pp. 101–133, Elsevier, Amsterdam, Oxford, New York, Tokyo (1989).
6. G. Demazeau, M. Pouchard, and P. Hagenmuller, *J. Solid State Chem.* **9,** 202 (1974).
7. P. M. Raccah and J. B. Goodenough, *Phys. Rev.* **155,** 932 (1967).
8. V. G. Bhide, D. S. Rajoria, Y. S. Reddy, G. Rama Rao, and C. N. R. Rao, *Phys. Rev. B* **8,** 5028 (1973).
9. D. S. Rajoria, V. G. Bhide, G. Rama Rao, and C. N. R. Rao, *J. Chem. Soc. Faraday Trans. 2* **70,** 512 (1974).
10. G. Demazeau, M. Pouchard, M. Thomas, J. F. Colombet, J. C. Grenier, L. Fournes, J. L. Soubeyroux and P. Hagenmuller, *Mater. Res. Bull.* **15,** 451 (1980); **16,** 533 (1981).
11. B. Buffat, G. Demazeau, M. Pouchard, and P. Hagenmuller, *Mater. Res. Bull.* **18,** 1153, 1983.
12. B. Buffat, G. Demazeau, R. Black, Y. Takeda, M. Pouchard, and P. Hagenmuller, *C. R. Acad. Sci. Paris* **295,** 557, 1982.
13. G. Demazeau, Thèse de l'Université Bordeaux I (France), no. 419 (1973).
14. F. Bertaut and F. Forrat, *J. Phys. Radium* **17,** 129 (1956).
15. A. Wold, B. Post, and E. Banks, *J. Am. Chem. Soc.* **79,** 4911 (1957).
16. M. Foex, A. Mancheron, and M. Line, *C. R. Acad. Sci. Paris* **250,** 3027 (1960).
17. G. Demazeau, M. Pouchard, and P. Hagenmuller, *J. Solid State Chem.* **18,** 159 (1976).
18. G. Demazeau, C. Parent, M. Pouchard, and P. Hagenmuller, *Mater. Res. Bull.* **7,** 913 (1972).
19. J. B. Goodenough, G. Demazeau, M. Pouchard, and P. Hagenmuller, *J. Solid State Chem.* **8,** 325 (1973).
20. G. Demazeau, I. Omeran, and M. Pouchard, *Mater. Res. Bull.* **11,** 1449 (1976).
21. K. Hayashi, G. Demazeau, M. Pouchard, and P. Hagenmuller, *Mater. Res. Bull.* **15,** 461 (1980).
22. J. Darriet, G. Demazeau, and M. Pouchard, *Mater. Res. Bull.* **16,** 1013 (1981).
23. O. Muller and R. Roy, *Mater. Res. Bull.* **4,** 39 (1969).
24. J. G. Bednorz and K. A. Müller, *Z. Phys. B-Condensed Matter* **64,** 189 (1986).
25. K. Yvon and M. Francois, *Z. Phys. B-Condensed Matter* **76,** 413 (1989).
26. Von B. Grande, Hk. Müller-Buschbaum, and M. Schweizer, *Z. Anorg. Allg. Chem.* **428,** 120 (1977).
27. Hk. Müller-Buschbaum and W. Wollschläger, *Z. Anorg. Allg. Chem.* **414,** 76 (1975).
28. M. K. Wu, J. R. Ashburn, C. J. Torng, P. H. Hor, R. L. Meng, L. Gao, Z. J. Huang, Y. Q. Wang, and C. W. Chu, *Phys. Rev. Lett.* **58** (9), 908 (1987).
29. H. Sawa, S. Suzuki, M. Watanabe, J. Akimitsu, H. Matsubara, H. Watabe, S. Uchida, K. Kokusho, H. Asano, F. Izumi, and E. Takayama-Muronachi, *Nature* **337,** 347 (1989).
30. H.-D. Wasel-Nielen and R. Hoppe, *Z. Anorg. Allg. Chem.* **375,** 43 (1970).
31. F. Abbattista, M. Vallino and D. Mazza, *J. Less-Common Met.* **110,** 391 (1985).

32. G. BLASSE, *J. Inorg. Nucl. Chem.* **27,** 2683 (1965).
33. R. V. PARISH, *in* "Mössbauer Spectroscopy Applied to Inorganic Chemistry" (G. J. Long, Ed.), Vol. 1, Chap. 17, p. 527, Plenum Press, New York (1984).
34. G. VILLENEUVE, T. ROJO, G. DEMAZEAU, AND P. HAGENMULLER, *Mater. Res. Bull.* **23,** 1787 (1988).
35. D. BALY AND K. PLIETH, *Z. Electrochem. Ber. Bun. Phys. Chem.* **59,** 55 (1955).
36. F. ABBATTISTA AND M. VALLINO, *Inorg. Chem. Acta* **140,** 147 (1985).
37. F. ABBATTISTA AND M. VALLINO, *Atti. Accad. Sci. Torino* **116,** 89 (1983).
38. F. ABBATTISTA AND M. VALLINO, *Mater. Res. Bull.* **20,** 293 (1985).